Preliminary Study of Single Particle Lidar for Wing Wake Survey

Matthieu VALLA, Béatrice AUGERE, Didier BAILLY, Agnès DOLFI-BOUTEYRE, Eric GARNIER, Michael MEHEUT
ONERA
Chemin de la hunière Palaiseau 91761 Cedex
FRANCE
matthieu.valla@onera.fr, beatrice.augere@onera.fr, didier.bailly@onera.fr
agnes.dolfi-bouteyre@onera.fr, eric.garnier@onera.fr, michael.meheut@onera.fr

1. Introduction

In this paper we assess the feasibility of an airborne lidar dedicated to wing wake survey, an application that would be of real interest for applied aerodynamics research. In flight wing wake survey could lead to non intrusive global drag estimation under realistic conditions.

Single particle coherent Doppler lidar (see Ref 1.) has proved to be efficient for measurements at high altitude (see Ref 2.), and thus, seems to be a good candidate to meet this challenge. The feasibility study focused on two main issues:

- Since wind speed is retrieved from the Doppler frequency shift of natural aerosol crossing the laser beam, the lidar introduces a bias in the measurement of the wing wake profile.
- Since the flow to be analyzed is turbulent, we have to evaluate the impact of aero optical effects upon lidar performances.

2. Lidar Bias Assessment

For wing wake survey, lidar raw data are used to compute the x component of flow velocity. Given the geometry of the lidar scan, other components (y and z) of the wing wake windfield have an influence over the radial velocity being measured by the lidar and, thus, introduce a bias.

Figure 1 shows a typical geometry: a lidar is installed inside a pod on the top of a wing. In this example, three distances from the trailing edge of the wing are considered. For global drag estimation, measurement distances lower than half wing chord are excluded because of a flow pressure becoming too different from the upstream static pressure value, leading to erroneous global drag estimates. Distances higher than one and a half chord are also excluded because of optical design constrains.

As seen in Figure 1, the laser axis differs from the x axis. The expected measurement span coordinate is reached thanks to an angle in the XY plane noted θ. The value of this angle is dependant on the expected measurement distance from the trailing edge of the wing. A vertical scan angle is also used in order to obtain the expected vertical dynamic for the wake measurement.

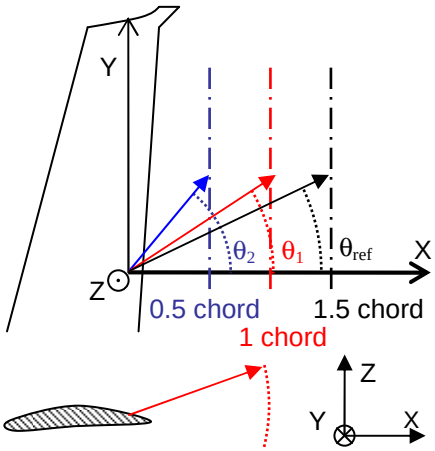

Figure 1: Lidar Geometry

In order to assess lidar geometrical bias, ONERA used 2.5 D Onera-elsA CFD (Computational Fluid Dynamics) RANS (Reynolds-Averaged Navier Stokes) sofware (see Ref 3.). The x component of the wing wake given by lidar was evaluated using the following steps:

- Radial velocity along the laser axis is computed from the whole wind speed vector with respect to the geometry of the lidar scan.
- The x component of the wing wake is then estimated from lidar data by compensating the angular projection between the lidar laser axis and the aircraft x axis.

Figure 2 shows wake profile measurements at two different distances from the trailing edge. The red plain line illustrates the real value of the x component of the flow;

and the green dash-dot line illustrates the x component estimated from lidar data.

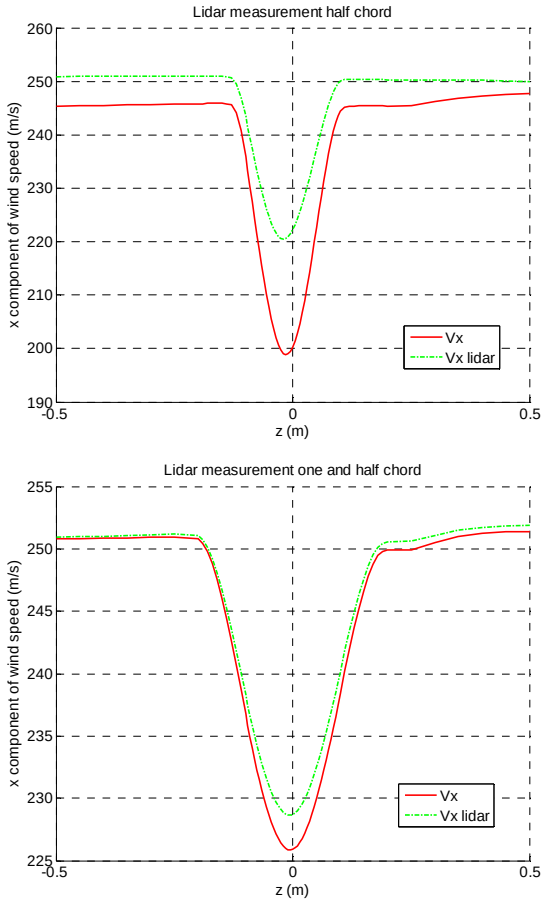

Figure 2: Wake Profile Measurements

The wake profile is characterized by a large downward bump centered around 0 m (consequence of the viscous wake), and a small downward bump around 0.25 m (consequence of the shock wave).

The results are consistent with the fact that the higher the angle between the laser axis and the x axis, the higher the lidar bias.

Despite the bias introduced by lidar geometry, drag extraction techniques (see Ref 4.) applied to lidar data give interesting results summarized in Table 1. Predictions of Cx coefficient from lidar data are obtained by both 1st order and Jones formulations. Those results are computed for various configurations, with different Mach numbers, different flow behaviors (partly laminar and fully turbulent) and at different measurement distances from the trailing edge. Results of drag are also directly computed from simulated wind field data using FFD (Fast Fluids Dynamics) code (see Ref 5.).

Results from Table 1 show that drag coefficient can be quite accurately predicted from lidar data.

	Mach	***FFD***	***LIDAR*** ***Cx 1st order*** ***Cx Jones*** ***x/c = 0,5 / 1,0 / 1,5***
Prescribed Transition	0.73	70	67 / 64 / 62 63 / 61 / 60
	0.75	59	57/ 54 / 53 53 / 51 / 49
	0.77	81	77 / 74 / 73 72 / 71 / 69
Fully Turbulent	0.73	101	100 / 94 / 91 94 / 91 / 91
	0.75	105	102 / 96 / 93 96 / 93 / 92
	0.77	113	111 / 106 / 101 104 / 102 / 100

Table 1: Drag extraction results

3. Aero optical effects assessment

Aero optical effects arise when the flow is turbulent: air density can no longer be considered constant and lead to variation of the refractive index of air (given by Gladstone-Dale's law). Laser beam propagation is disturbed in such a turbulent medium, resulting in loss of lidar performance: the laser beam can not be focused as tight as it should be in order to ensure a power budget suitable for single particle detection.

The coherent lidar community has experience concerning turbulent propagation of laser beam caused by natural heat convection (see Ref 6.), a phenomenon common for ground based lidar. It was found that a full aero optical assessment (i.e. simulating samples of air density turbulence and the corresponding phase screen propagation) required computer intensive simulations that were out of scope of ONERA preliminary work.

ONERA made a preliminary assessment (close to Ref 7. approach) based on RANS simulations and laser propagation in heat induced turbulence theory. We made the assumption that aero optical induced turbulence is isotropic, locally homogenous within the laser beam scale, and characterized by the following refractive index spectrum:

$$\Phi_{n_1}(k) = \frac{K^2 \sigma_\rho^2 \Gamma(11/6)}{\left(2\pi L_0^2\right)^{1/3} \Gamma(3/2)\Gamma(2/6)} \left(k^2 + 4\pi^2 L_0^{-2}\right)^{-11/6}$$

Where K is the Gladstone-Dale constant for air, σ_ρ^2 the air density variance, and L_0 the large scale of turbulence.

This formulation of the refractive index spectrum is explicitly dependant on air density variance, and implicitly dependant on air density correlation length (Lρ) via the large scale of turbulence.

RANS computations do not give direct access to these quantities and further assumptions are needed for their evaluation. Aupoix (see Ref 8.) has proposed to quantify the air density fluctuations as follows:

$$\sigma_\rho = \frac{k}{\mathrm{Pr}_t^{\,2}} \left(\frac{\left(\frac{d\rho}{dz} \right)}{\left(\frac{du}{dz} \right)} \right)^2$$

Where ρ is the air density and u the x component of the flow speed.

This formula is based on approximations only reliable in a 2D boundary layer flow. These flows share with wake flows of interest in this study the property of having only one direction on strong variation (z). Nevertheless, it is important to notice that such an evaluation of density fluctuations has never been validated experimentally in a wake. Moreover, it has to be regularized in order to avoid local divergence when velocity gradient cancels out.

The correlation length of the density (Lρ) is evaluated doing two strong assumptions:

- The correlation length of the density is the same as the one of the velocity.
- The correlation of the velocity is isotropic.

Doing so, it is possible to associate Lρ with the integral length given by a turbulence model. In particular, it is a direct output of k-l model.

Figure 3 illustrates the air density variance and coherence length, derived from RANS computations downstream from the trailing edge (the trailing edge being localized at the origin). One should note that, concerning the air density coherence length, the values given in Figure 3 are only meaningful in the turbulent part of the flow (the wing wake).

Values of refractive index structure parameter C_n^2 estimated from RANS simulations were found to be in the highly turbulent order of magnitude concerning laser propagation, $C_n^2 \approx 1.10^{-12}\ m^{-2/3}$.

This level of turbulence is in the same order of magnitude than turbulence caused by the boundary layer near the lidar window, with a noticeable difference: the propagation distance inside the turbulent wake is much higher than the thickness of the boundary layer.

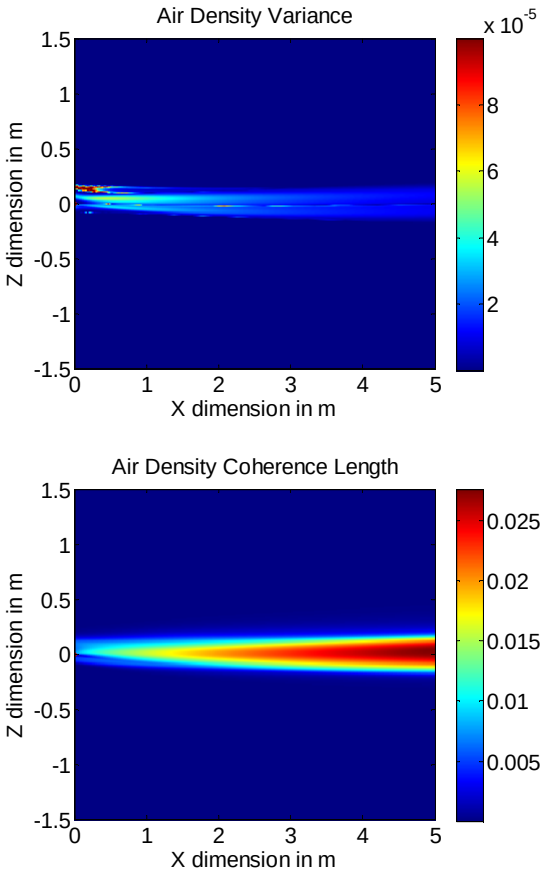

Figure 3: Air Density Variance and Coherence

Computing lidar performance (i.e. number of particles detected per second) leads to the results presented in Figure 4. The number of particles detected per second is computed versus lidar footprint (i.e. laser beam radius) at different locations ranging from half chord to one and a half chords away from the trailing edge.

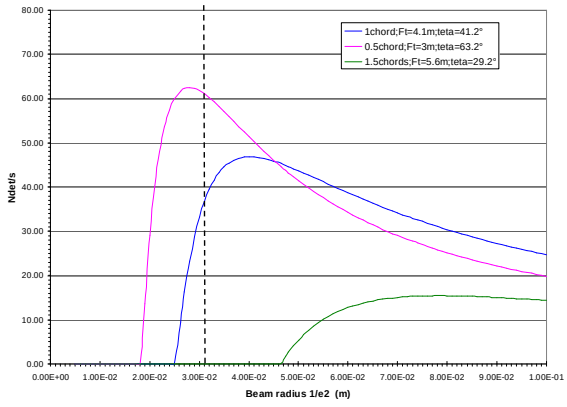

Figure 4: Lidar Performance

The lidar footprint can not be extended to infinity and a reasonable upper limit is shown by the vertical dashed line.

Here again the results are consistent with the fact that the longer the propagation path, the higher the penalty on lidar performance.

This preliminary aero optical effect assessment shows that measurements at half chord and one chord downstream of the trailing edge are still possible, whereas the measurement at one and half chords is not possible.

However, we consider that model uncertainties (density and size distribution of particles, real value of Gladstone-Dale constant for air at such pressure, temperature and laser wavelength) are high enough so that measuring at one chord is taking high risks.

4. Conclusion

We can conclude that, because of uncertainties regarding aero optical effects, Single particle coherent Doppler lidar for wing wake survey has to go through a proof of concept.

Preliminary airborne trials should be undertaken with a very similar configuration: installing a lidar inside an aircraft cabin doing wake measurements of the root of the wing.

5. Acknowledgements

This work has been undertaken within the Joint Technology Initiative "JTI CleanSky", Smart Fixed Wing Aircraft Integrated Technology Demonstrator "SFWA-ITD" project (contract N° CSJU-GAM-SFWA-2008-001) financed by the 7th Framework programme of European Commission.

6. References

1. M. Harris, G. N. Pearson, K. D. Ridley, C. J. Karlsson, F. A. Olsson, D. Letalick, ‘ Single-Particle Laser Doppler Anemometry at 1.55 µm ‘, Applied Optics, Vol. 40, No. 6, pp. 969-973 (2001).
2. T. Katsibas, T. Semertzidis, X. Lacondemine, N. Grammalidis, ‘ Signal Processing for a Laser Based Air Data System In Commercial Aircrafts ’, 16th European Signal Processing Conference (EUSIPCO 2008), Lausanne, Switzerland.
3. L. Cambier, J.P. Veuillot, ‘ Status of the elsA Software for Flow Simulation and Multi-Disciplinary Applications ‘, 46th AIAA Aerospace Sciences Meeting and Exhibit, Reno, Nevada, January 7-10, 2010.
4. M. Méheut, D. Bailly, ‘ Drag-Breakdown Methods from Wake Measurements ’, AIAA Journal, Vol. 46, No. 4, pp. 847-862, April 2008.
5. D. Destarac, ‘ Drag Extraction from Numerical Solutions to the Equations of Fluid Dynamics: the Far-field “Philosophy” ‘, 43ème Congrès d’Aérodynamique Appliquée de la 3AF, Maîtrise de la traînée et de l’impact sur l’environnement, Poitiers, 10-12 Mars 2008.
6. R. G. Frehlich and M. J. Kavaya, ‘ Coherent Laser Radar Performance for General Atmospheric Refractive Turbulence ’, Applied Optics, Vol. 30, No. 36, pp. 5325–5352 (1991).
7. E. Frumker, O. Pade, ‘ Generic Method for Aero-Optic Evaluations ’, Applied Optics, Vol. 43, No. 16, pp. 3224-3228 (2004).
8. B. Aupoix, ‘ Prévision des Effets Aéro-Optiques en Couche Limite ‘ Internal Technical Report RT1/07893 DMAE, 2003, Onera, France.